



**15<sup>th</sup> Canadian Masonry Symposium**  
**Ottawa, Canada**  
**June 2-5, 2025**



---

**Climate Change Impact on Built Environment:  
Definition of Surrogate Vulnerability Models**

**Sara Mozzon<sup>i</sup>, Marco Donà<sup>ii</sup>, Michol Rampado<sup>iii</sup>, and Francesca da Porto<sup>iv</sup>**

**ABSTRACT**

The built environment, particularly buildings, is susceptible to both structural and economic damage caused by a wide range of catastrophic events, including earthquakes, floods, landslides, debris flows, hurricanes, and tsunamis. In recent decades, the intensity and frequency of some of these natural hazards have increased due to ongoing climate change. Consequently, there is a growing need to investigate the effects of multiple interacting hazards and to adopt a multi-risk perspective. However, to date, the various metrics used in risk assessment for individual hazards are generally not comparable. Therefore, as a first step toward a comprehensive multi-risk evaluation, a multilayer assessment framework integrating different risks represents a significant contribution.

Italy is among the countries most affected by natural disasters, highlighting the importance of multidisciplinary approaches for developing multi-vulnerability models that estimate the impacts of such events on the built environment. The predominant structural types of residential buildings in Italy include unreinforced masonry and reinforced concrete, mainly in the form of frames with brick infill. To address this, an analytical model was developed to assess the out-of-plane response of masonry elements such as load-bearing walls and infill panels. The model simulates a dual arching mechanism within the wall thickness using an incremental procedure with out-of-plane displacement control. This model was then integrated into a Monte Carlo simulation, allowing for variability in both the geometric and mechanical properties of walls, which were previously classified into different categories. Finally, a surrogate vulnerability model was derived from the Monte Carlo results.

**KEYWORDS**

Climate change impact, masonry wall, Monte Carlo analysis, surrogate vulnerability models.

---

<sup>i</sup> PhD candidate, Department ICEA, University of Padova, Padova, Italy, sara.mozzon@unipd.it

<sup>ii</sup> RTDb, Department of Geosciences, University of Padova, Padova, Italy, marco.dona.l@unipd.it

<sup>iii</sup> PhD student, Department of Geosciences, University of Padova, Padova, Italy, michol.rampado@phd.unipd.it

<sup>iv</sup> Full Professor, Department of Geosciences, University of Padova, Padova, Italy, francesca.daporto@unipd.it



## **INTRODUCTION**

Geological, hydrological, and hydraulic instability phenomena are widespread in Italy, causing significant damage and posing serious threats to the population, infrastructure, environment, and buildings [1,2]. In recent years, several catastrophic events have resulted in substantial destruction and loss of life. A global dataset [3] estimates that between 1998 and 2023, Europe experienced over 500 major damaging floods. Floods are among the most frequent and costly natural disasters worldwide [4], highlighting the urgent need for coordinated risk management strategies [4,5]. As noted by [6,7], flash floods and debris flows pose severe risks, particularly in mountainous regions, where they can be triggered by intense rainfall or dam failures, with devastating consequences downstream. These risks are exacerbated by factors such as hydraulic infrastructure degradation, climate change-driven hydrological intensification, and increased exposure due to urban expansion [7,8]. Effective flood and debris flow risk assessment is therefore crucial for designing both structural and non-structural mitigation strategies.

A comprehensive risk assessment must integrate hazard, vulnerability, and exposure [7]. However, in practice, risks from different hazard sources are often evaluated separately. To address this limitation, transitioning towards a unified multi-risk framework is essential for assessing the combined impact of multiple hazards within a given area [9,10]. The goal is to establish a consistent methodology that accounts for interactions between natural processes. As a preliminary step, a multi-layer vulnerability evaluation can be conducted, assessing individual hazards independently while harmonizing and standardizing vulnerability assessment procedures [1]. Assessing the vulnerability of the built environment, particularly in areas prone to multiple natural hazards, is critical due to the severe consequences of structural damage to buildings, and in extreme cases their collapse, can have on human life [11,12]. A robust understanding of vulnerability enhances risk assessment, improves emergency management, and supports mitigation and preparedness strategies, ultimately reducing both economic losses and human casualties [13]. Several studies have focused on the vulnerability of masonry [4,12,14-16] and reinforced concrete [17,18] structures subjected to horizontal hydraulic and debris actions.

In Italy, the predominant structural types of residential buildings are unreinforced masonry (URM) and reinforced concrete (RC) with brick infill panels. URM buildings rely on load-bearing walls, meaning the collapse of a single wall can compromise overall stability. RC buildings, composed of frames with infill panels, which are particularly susceptible to out-of-plane horizontal actions. A local-type stability analysis [12] of individual structural (load-bearing walls) and non-structural (infills) elements provides a rational approach for evaluating the effects of natural events such as flash floods and debris flows, which are increasing due to climate change [11].

This paper presents an analytical model developed to assess the out-of-plane response of masonry load-bearing walls and infill panels, considering both simple and reinforced masonry. The model was implemented in a Monte Carlo simulation, incorporating variations in geometric and mechanical properties across different wall classifications. Based on the Monte Carlo results, polynomial surrogate vulnerability models were derived to describe the out-of-plane behavior of walls and infill panels, providing an efficient tool for vulnerability assessment.

## **PRESENTATION OF THE ANALYTICAL MODEL**

The analytical model, presented in this paper, simulates a plate resistance mechanism, incorporating the development of a double arching mechanism (vertical and horizontal) within the wall thickness. This is combined with an incremental procedure that controls out-of-plane (OOP) displacements. The code iteratively calculates equilibrium by applying horizontal forces and recalibrating the balance of forces and

moments until wall collapse occurs. As shown in Fig. 1, cracks (in red) develop along five internal fracture lines, dividing the wall into four blocks.

The model is highly adaptable, as it allows for the analysis of walls subjected to horizontal load profiles of varying shapes (triangular, rectangular and trapezoidal) and heights ( $h_w$ ), enabling the simulation of different types of events. Additionally, it can be integrated into a Monte Carlo simulation to derive capacity models for different wall types, accounting for uncertainties in geometric and mechanical parameters. From a multi-risk perspective, the model is designed to align with other established methodologies, such as those used for seismic risk assessment, enhancing its applicability across various hazard scenarios.

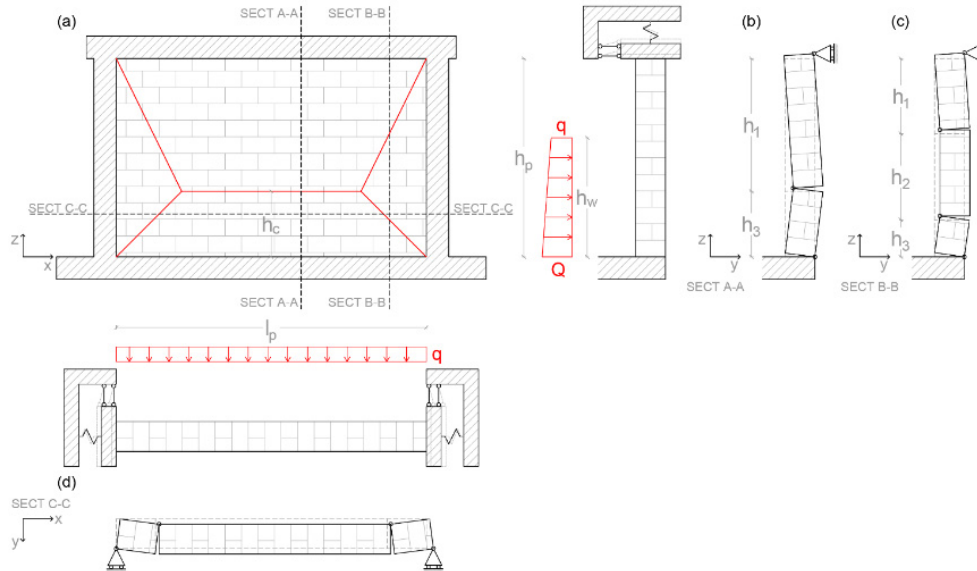


**Figure 1: Possible failure mechanism of a wall subjected to trapezoidal-shaped horizontal actions (combining hydrostatic and hydrodynamic effects): (a) front view, (b) flat cross section, (c) and (d) vertical cross sections.**

### Key features of the model

The main assumptions of the analytical model are as follows:

- Plate-like behavior. In line with [12,15], a primary failure mechanism involves the formation of five internal fracture lines, dividing the wall into four blocks. Once the first fracture line develops, the wall is further subdivided into three segments near the perimeter constraints and two segments in the central area (alternative configurations will be presented in future works).
- Position of the horizontal fracture line. The horizontal fracture line is assumed to develop where the external load profile induces the maximum bending moment in the wall.
- Development of a dual arching mechanism through the wall thickness. Due to the low tensile strength of masonry, especially after cracking, many out-of-plane strength models in the literature rely on an arching mechanism (or compressed strut). This is justified by the negligible contribution of masonry's flexural strength to overall resistance. The assumption aligns with the standard approach outlined in [19].

- Rigid rotation of the segments. The application of an out-of-plane displacement along the horizontal fracture line induces a rigid rotation of the segments around cylindrical hinges at the fracture lines. For simplicity, the analytical model assumes no relative slip between adjacent segments [12].
- Deformation along the segment height. The deformations of the external segments (i.e., the upper and lower parts of the wall) follow a triangular distribution along their height, with a maximum value at the cylindrical hinge section and zero at the opposite end.
- Finite stiffness of surrounding beams and columns. The model accounts, for the case of infill panels, for the vertical deformability of the top beam in the vertical arching mechanism and the horizontal deformability of the columns in the horizontal arching mechanism.
- Effect of vertical loads. In load-bearing masonry walls, the vertical arching mechanism also considers the effect of vertical loads from floors and upper walls, along with the contribution of the wall's self-weight.
- Non-linear stress-strain behavior of materials. (a) The compressive strength of masonry and any reinforcing layers (e.g., plaster) follows an elasto-plastic law with a softening branch. The stress-strain curve is trapezoidal, consisting of an initial elastic section, a plateau representing the plastic phase, and a softening section with a constant negative slope, stabilizing at a residual stress level. (b) The tensile behavior of any external reinforcement follows an elasto-plastic law, while masonry tensile strength is assumed to be zero.

### OOP capacity curves of load-bearing walls and performance points

This section presents the OOP capacity curves obtained for a main load-bearing masonry wall. Specifically, the analysis considers a wall oriented orthogonally to the span of the horizontal diaphragms, thereby supporting floor loads. The wall is constructed using solid blocks with double headers and lime mortar.

The following curves refer to the case of a main load-bearing wall supporting a wooden floor (with an influence length of 3.00 m) subjected to a load of  $g_1+g_2=1.50\text{kN/m}^2$ . For a fixed load height of  $h_w = 2.00\text{m}$ , Fig. 2 (left) illustrates the development of the vertical arch OOP capacity for different horizontal load distributions, characterized by varying load shape constants  $k$  (where  $k=1$  corresponds to a rectangular load shape and  $k=0$  to a triangular load shape). The lowest capacity is observed when the load shape is rectangular. Accordingly, Fig. 2 (right) displays the vertical arch capacity curves obtained for a rectangular load shape while varying the impacted wall ratio ( $h_w/h_p$ ).

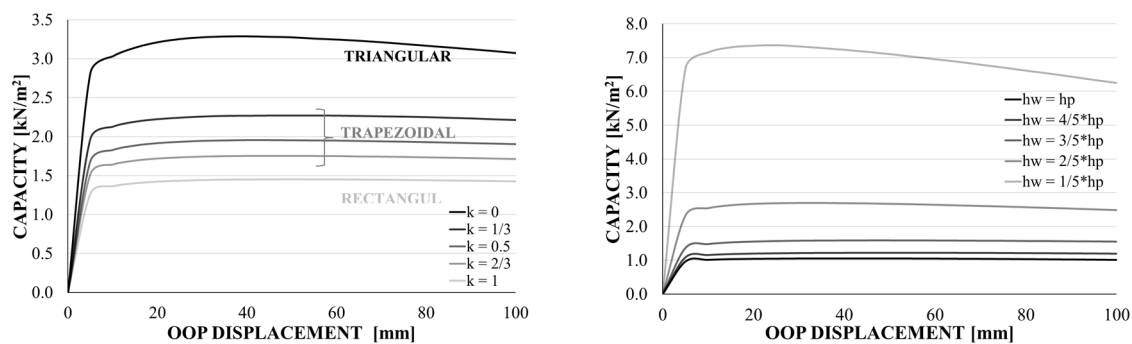


**Figure 2: OOP capacity curves of the load-bearing wall for different load profile shapes at a fixed load height (left), and for rectangular load profiles with varying impacted wall ratios (right).**

Furthermore, as shown in Fig. 3, three distinct performance points can be identified on the capacity curves, providing a characterization of the out-of-plane response of the investigated wall. The first performance point corresponds to the onset of cracking, which is identified on the capacity curve by comparing the computed capacity with the moment value obtained from Navier’s formula. The second performance point represents a moderate damage state. Finally, the third performance point is reached when the wall attains its maximum out-of-plane capacity.

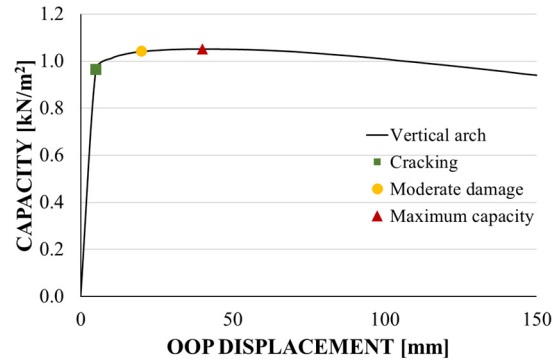


**Figure 3: Performance points identified on the capacity curve of the vertical arch for the load-bearing wall, obtained for a rectangular load profile ( $h_w = 3.00\text{m}$ ).**

## PROPOSAL OF SURROGATE VULNERABILITY MODELS

To fully exploit the versatility of the analytical model presented in the previous section, it is crucial to establish a comprehensive taxonomy of the wall elements under investigation. This required an initial classification based on the functional role of these elements, distinguishing between two macro-categories: (i) non-structural walls and (ii) structural walls. The first category includes infill panels located within the envelopes of reinforced concrete frame buildings. The second category comprises load-bearing masonry walls, which can be further divided into main walls – those oriented orthogonally to the span of the horizontal diaphragms and supporting floor loads – and secondary walls, which are oriented parallel to the diaphragm span. Each macro-category is further subdivided into various classes based on construction techniques, which differ in terms of mechanical properties, geometric dimensions, and the characteristics of the masonry units.

To account for the uncertainties – both stochastic and epistemic – associated with the key parameters defining each wall class, a Monte Carlo simulation was performed. This approach ensures that the results are applicable to risk assessments at a territorial scale, where detailed information about building exposure is often limited or unavailable.

To characterize the out-of-plane response of the wall elements under investigation, point clouds representing wall capacity at key performance points were generated for each wall class and type of lateral action. Given the large dataset produced, surrogate vulnerability or capacity models were defined and calibrated to enable a direct assessment of these capacity values. This process led to the formulation of three second-degree polynomial equations – one for each identified performance point – specific to each wall class and lateral load configuration.

### Taxonomy of structural masonry elements

The first step of the analysis involved identifying two primary classes of elements based on their structural function: non-structural and structural walls. The former includes infill panels, further classified into sub-classes according to their geometric dimensions and whether they belong to existing buildings or new

constructions. Additionally, a further distinction is made based on the size and mechanical properties of the blocks composing the panels. The second class comprises load-bearing masonry walls, which are similarly divided into sub-classes based on the characteristics of the masonry units and whether they pertain to existing masonry buildings or newly constructed ordinary masonry structures. For this classification, the subdivision of masonry types proposed in [20] was adopted as a reference.

As an example, Tab. 1 provides the geometric properties (based on [21,22] and visual references) and mechanical properties (based on [23]) for the sub-class of load-bearing masonry made with single-headed solid bricks and lime mortar. These properties are essential for defining the wall behavior and for calibrating the surrogate vulnerability models.

**Table 1: Main characteristics of the load-bearing wall selected sub-class.**

Existing constructions	Value range of key parameters		
	Wall geometry	Masonry unit size	Mechanical properties
Single-headed solid bricks and lime mortar masonry	$h_p = 2.5 \div 3.5\text{m}$ $l_p = 2.5 \div 6.0\text{m}$ $t_p = 0.12\text{m}$	$h_b = 0.055\text{m}$ $l_b = 0.25\text{m}$ $t_m = 0.01\text{m}$	$f_v = f_h = 2.6 \div 4.3\text{MPa}$ $E_v = E_h = 1200 \div 1800\text{MPa}$

### Monte Carlo simulation

The analytical model developed and described in the previous section can be integrated into a Monte Carlo simulation to generate point clouds representing the capacity of various infill/wall classes, corresponding to selected performance points of the out-of-plane (OOP) behavior. These point clouds serve as the foundation for developing capacity models for load-bearing masonry walls and infill panels.

The Monte Carlo analysis is a crucial component in simulation modeling, as it allows for the examination of uncertainties and variabilities inherent in complex systems. In this case, it facilitates the incorporation of uncertainties related to key parameters, including:

- geometric parameters (e.g. shape ratio, slenderness, blocks and/or bricks dimensions, etc.)
- mechanical parameters (such as, e.g., material strengths, stiffness modulus, stiffness of the external supports/bonds, characteristics of any reinforcements, etc.).

At its core, the Monte Carlo analysis utilizes random sampling and statistical modelling to approximate the behaviour of deterministic systems under uncertain conditions. The first step in developing a Monte Carlo analysis is to define the problem and identify the key variables that influence the model's behavior. Once the relevant parameters are identified, appropriate probability distributions are assigned to these variables. The choice of distribution is crucial, as it directly impacts the accuracy and reliability of the simulation results. After establishing the probability distributions, random samples are generated for each variable. These samples are then used to perform multiple iterations of the model, each representing a potential scenario for the system's behavior. Typically, thousands or even millions of simulations are run to ensure a statistically robust representation of the possible outcomes.

In this study, a uniform random distribution of values between the minimum and maximum values (provided in Tab. 1) was selected for the geometric parameters. For the mechanical properties, a lognormal distribution was used, with the mean ( $\mu$ ) and standard deviation ( $\sigma$ ) calculated according to the methodology described in [23].

### Surrogate vulnerability models' coefficients of load-bearing walls class

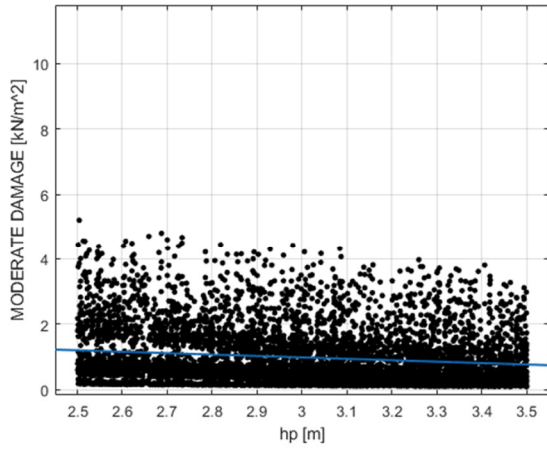
Once the point clouds for each performance point of the various sub-classes of load-bearing walls were obtained – considering both rectangular and triangular load shapes – appropriate surrogate capacity models were defined and calibrated based on these results. These models can still be referred to as surrogate vulnerability models, as they also account for the characteristics of the flood action, including the profile shape and loading height. In addition to providing a concise summary of the extensive numerical analysis conducted, these models enable the direct evaluation of capacity values at different performance points for the various wall classes, using simple second-degree polynomial equations.

The choice of a polynomial model was based on a trade-off between predictive accuracy and simplicity. Specifically, a preliminary analysis was conducted to assess the influence of key study parameters (i.e., the variables in the Monte Carlo analysis) on capacity values. For masonry load-bearing walls, six main parameters were identified as governing capacity: the height of the infill panel ( $h_p$  [m]), the inverse of its slenderness ( $t_p/h_p$  [-]), its aspect ratio ( $l_p/h_p$  [-]), the impacted infill ratio ( $h_w/h_p$  [-]), the average compressive strength of masonry ( $f_m$  [MPa]), and the floor load ( $g_{floor}$  [MPa]). As with infill panels, these parameters influence capacity either individually (through linear or quadratic relationships) or in combination.

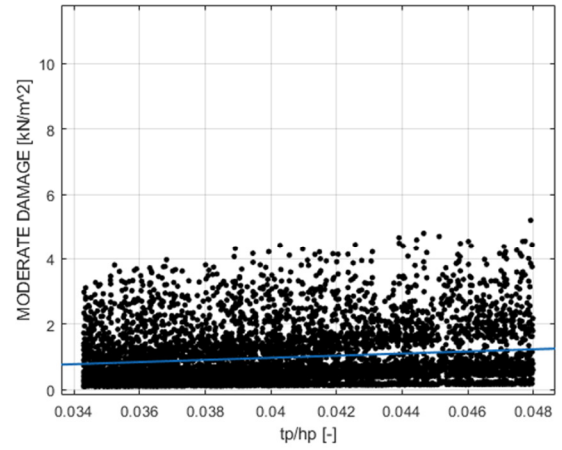
For individual dependencies, height, inverse slenderness, aspect ratio, mean compressive strength, and floor load were found to influence wall capacity in a linear manner. In contrast, the impacted wall ratio exhibited a non-linear effect, necessitating a quadratic dependency. Additionally, combined dependencies were observed between the impacted wall ratio and other parameters, such as height, inverse slenderness, aspect ratio, and floor load, which could reasonably be approximated as linear. Accordingly, the surrogate vulnerability model for masonry load-bearing walls takes the following general form:

$$(1) \text{ CAPACITY} = c_0 + c_1 \cdot h_p + c_2 \cdot \frac{t_p}{h_p} + c_3 \cdot \frac{l_p}{h_p} + c_4 \cdot f_m + c_5 \cdot g_{floor} + c_6 \cdot \frac{h_w}{h_p} + c_7 \cdot \left(\frac{h_w}{h_p}\right)^2 + c_8 \cdot h_p \cdot \frac{h_w}{h_p} + c_9 \cdot \frac{t_p}{h_p} \cdot \frac{h_w}{h_p} + c_{10} \cdot \frac{l_p}{h_p} \cdot \frac{h_w}{h_p} + c_{11} \cdot g_{floor} \cdot \frac{h_w}{h_p}$$

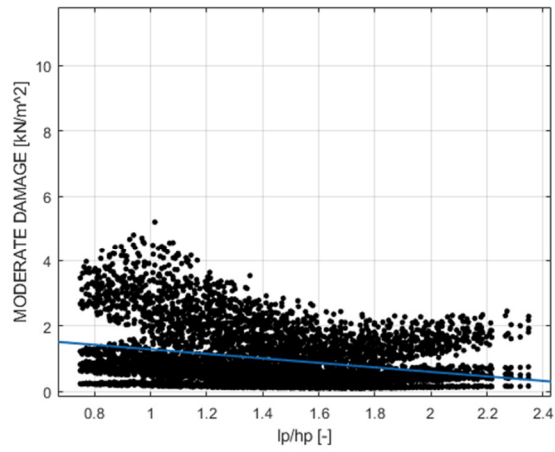
The results presented here pertain to the sub-class of load-bearing walls constructed with single-headed bricks (12cm wall thickness) and lime mortar. For brevity, the discussion is limited to the case of a rectangular-shaped load profile; however, similar trends are observed for triangular-shaped load profiles. Fig. 4 illustrates the variation in maximum capacity values of the masonry walls in the case study class as a function of key study parameters, while Fig. 5 depicts the combined dependencies between the impacted wall ratio and the other primary parameters. Tab. 2 provides the calibration coefficients for the associated surrogate vulnerability model for a rectangular-shaped load. Tab. 3 reports the values of the  $R^2$  and adjusted  $R^2$  parameters, which indicate the fit of the polynomial surrogate model.



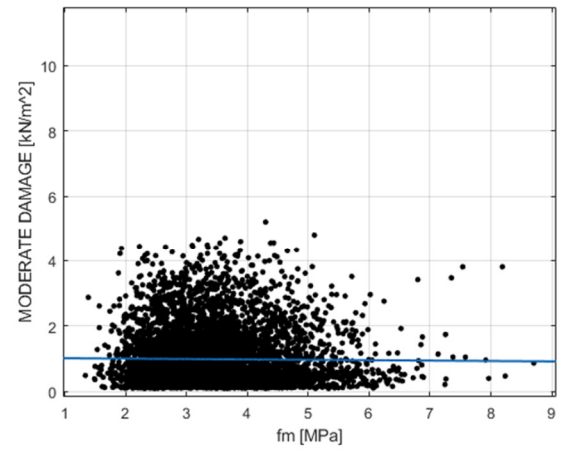
(a)



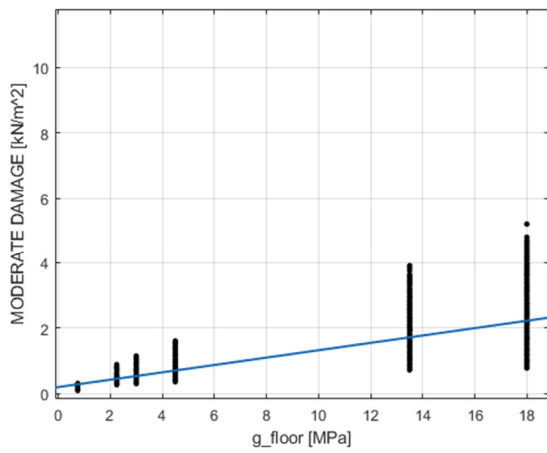
(b)



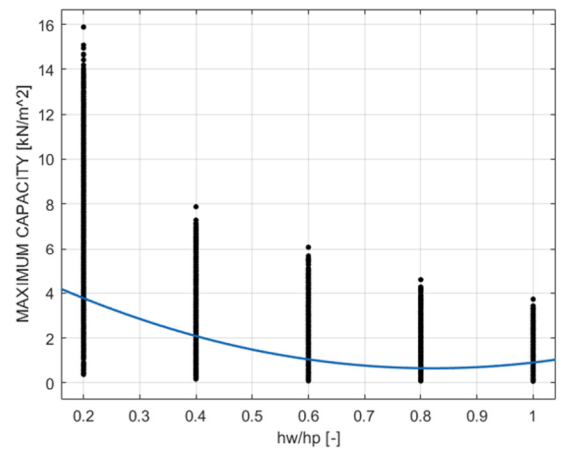
(c)



(d)



(e)



(f)

**Figure 4: Maximum capacity of case study walls: individual dependences on key parameters.**

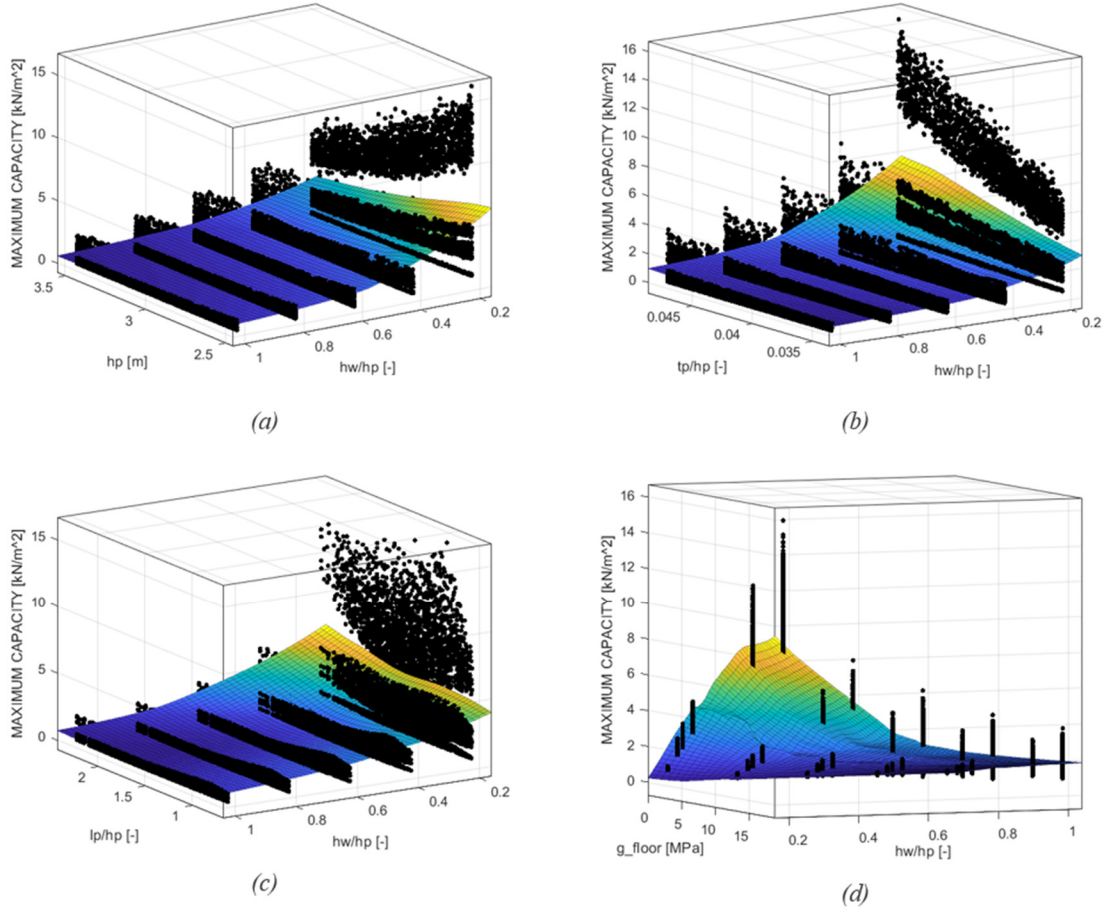


**Figure 5: Maximum capacity of case study walls: combined dependences on key parameters.**

**Table 2: Coefficients of the surrogate vulnerability model of the selected wall class, for rectangular-shaped load.**

Variables	Coef. name	Coef. values (rectangular-shaped load)		
		First cracking	Moderate damage	Maximum capacity
Intercept [-]	$c_0$	-6.03E+00	-4.34E+00	-2.66E+00
$h_p$ [m]	$c_1$	8.78E-01	6.28E-01	3.78E-01
$t_p/h_p$ [-]	$c_2$	1.68E+02	1.34E+02	9.88E+01
$l_p/h_p$ [-]	$c_3$	-7.54E-01	-7.33E-01	-7.13E-01
$f_m$ [MPa]	$c_4$	-3.57E+00	-2.56E+00	-1.55E+00
$g_{floor}$ [MPa]	$c_5$	2.15E-01	1.42E-01	6.85E-02
$h_w/h_p$ [-]	$c_6$	5.21E-01	-2.89E-02	-5.79E-01
$(h_w/h_p)^2$ [-]	$c_7$	-1.92E-03	-1.38E-03	-8.32E-04
$h_p (h_w/h_p)$ [m]	$c_8$	-8.08E-02	9.76E-03	1.00E-01
$(t_p/h_p) (h_w/h_p)$ [-]	$c_9$	-6.55E+00	2.48E-01	7.05E+00
$(l_p/h_p) (h_w/h_p)$ [-]	$c_{10}$	-4.92E-04	-7.36E-04	-9.80E-04
$g_{floor} (h_w/h_p)$ [MPa]	$c_{11}$	-5.51E-04	-3.39E-04	-1.27E-04

**Table 3: Goodness of fit of the polynomial models.**

Surrogate vulnerability model	Rectangular-shaped load	
	R2	Adjusted R2
First cracking	0.64	0.64
Moderate damage	0.70	0.70
Maximum capacity	0.67	0.67

## CONCLUSIONS

Based on the taxonomy established for structural and non-structural masonry elements, a Monte Carlo simulation was performed by iteratively applying the analytical model presented in this paper. This approach enabled the assessment of the out-of-plane capacity of masonry infills and walls while accounting for potential variations in their key geometric and mechanical parameters. Consequently, it allowed for the inclusion of both epistemic and aleatory uncertainties for each infill and wall class, yielding capacity results suitable for vulnerability assessments at a territorial scale, where detailed building exposure data is often scarce.

Specifically, the Monte Carlo simulation generated point clouds representing the capacity of infills/walls at selected performance points – namely, first cracking, moderate damage, and maximum capacity – for each investigated infill/wall class and load profile shape. In general, the capacity values rise with decreasing height and slenderness of the wall. For load-bearing walls, the floor load has a clear stabilizing effect on the out-of-plane capacity, contributing to the overall rotational equilibrium of the wall.

Following the Monte Carlo simulation and the generation of a substantial dataset, surrogate vulnerability models were defined and calibrated against these results. These models allow for the direct estimation of the infill/wall capacity associated with a specific performance point and a given lateral load shape. Specifically, three polynomial equations – one for each selected performance point – were formulated for each wall/panel class, separately for rectangular and triangular load shapes. In the case of load-bearing walls, these equations were expressed as functions of six key parameters: panel height, inverse of slenderness, aspect ratio, impacted infill ratio, mean compressive strength of masonry, and the floor load. Furthermore, for wall classes with variable masonry unit sizes, additional parameters such as wall thickness and the height-to-width ratio of the masonry unit were included.

## ACKNOWLEDGEMENTS

This study was carried out within the RETURN Extended Partnership and received funding from the European Union Next-GenerationEU (National Recovery and Resilience Plan – NRRP, Mission 4, Component 2, Investment 1.3 – D.D. 1243 2/8/2022, PE0000005).

The authors would also like to express their sincere gratitude to the Italian Department of Civil Protection and the ReLUIs consortium for their valuable support in the development of this work, carried out within the ReLUIs-DPC 2024–2026 Project, Work Package 3 (Tasks 3.1, 3.2, 3.3, and 3.5).

## REFERENCES

- [1] Poljanšek, K., Marin Ferrer, M., De Goeve, T., and Clark, I. (2017) Science for disaster risk management 2017 knowing better and losing less and losing less. Publications Office of the European Union, Luxembourg.
- [2] Spano, D., Mereu, V., Bacciu, V., Marras, S., Trabucco, A., Adinolfi, M., et al. (2020) Analisi del Rischio. I cambiamenti climatici in Italia.
- [3] (n.d.) EM-DAT - The international disaster database.

- [4] Capparelli, G., Liguori, F.S., Madeo, A., and Versace, P. (2023) A rapid numerical-based vulnerability assessment method for masonry buildings subject to flood. *International Journal of Disaster Risk Reduction*. 97 104001.
- [5] Bangalore, M., Hallegatte, S., Bonzanigo, L., Kane, T., Fay, M., Narloch, U., et al. (2016) *Shock Waves: Managing the Impacts of Climate Change on Poverty*. Washington, DC: World Bank.
- [6] Iverson, R., Ed. (2004) "Debris flow." In *Encyclopedia of geomorphology*, edited by A. Goudie, 225. Routledge, London.
- [7] Milanese, L. and Pilotti, M. (2021) Coupling Flood Propagation Modeling and Building Collapse in Flash Flood Studies. *Journal of Hydraulic Engineering*. 147 (12), 04021047.
- [8] Fuchs, S., Heiser, M., Schlögl, M., Zischg, A., Ppathoma-Köhle, M., and Keiler, M. (2019) Short communication: A model to predict flood loss in mountain areas. *Environmental Modelling and Software*. 117 176–180.
- [9] Marzocchi, W., Garcia-Aristizabal, A., Gasparini, P., Mastellone, M.L., and Di Ruocco, A. (2012) Basic principles of multi-risk assessment: a case study in Italy. *Natural Hazards*. 62 (2), 551–573.
- [10] IPCC, Ed. (2014) *Climate Change 2014: Synthesis Report. Contribution of Working Groups I, II and III to the Fifth Assessment Report of the Intergovernmental Panel on Climate Change* [Core Writing Team, R.K. Pachauri and L.A. Meyer (eds.)]. Intergovernmental Panel on Climate Change, Geneva, Switzerland.
- [11] Cantelmo, C. and Cuomo, G. (2021) Hydrodynamic loads on buildings in floods. *Journal of Hydraulic Research*. 59 (1), 61–74.
- [12] Milanese, L., Pilotti, M., Belleri, A., Marini, A., and Fuchs, S. (2018) Vulnerability to Flash Floods: A Simplified Structural Model for Masonry Buildings. *Water Resources Research*. 54 (10), 7177–7197.
- [13] Ppathoma-Köhle, M., Kappes, M., Keiler, M., and Glade, T. (2011) Physical vulnerability assessment for alpine hazards: State of the art and future needs. *Natural Hazards*. 58 (2), 645–680.
- [14] Asad, M., Thamboo, J., Zahra, T., and Thambiratnam, D.P. (2024) Out-of-plane failure analysis of masonry walls subjected to hydrostatic and hydrodynamic loads induced by flash floods. *Engineering Structures*. 298 117041.
- [15] Herbert, D.M., Gardner, D.R., Harbottle, M., and Hughes, T.G. (2018) Performance of single skin masonry walls subjected to hydraulic loading. *Materials and Structures/Materiaux et Constructions*. 51 (4),.
- [16] Lonetti, P. and Maletta, R. (2018) Dynamic impact analysis of masonry buildings subjected to flood actions. *Engineering Structures*. 167 445–458.
- [17] Petrone, C., Rossetto, T., and Goda, K. (2017) Fragility assessment of a RC structure under tsunami actions via nonlinear static and dynamic analyses. *Engineering Structures*. 136 36–53.
- [18] Luo, H.Y., Fan, R.L., Wang, H.J., and Zhang, L.M. (2020) Physics of building vulnerability to debris flows, floods and earth flows. *Engineering Geology*. 271 105611.
- [19] (2022) Eurocode 6 - Design of masonry structures - Part 1-1: General rules for reinforced and unreinforced masonry structures.
- [20] (2018) Aggiornamento Delle «Norme Tecniche per Le Costruzioni».
- [21] Boschi, S., Giordano, S., Signorini, N., and Vignoli, A. (n.d.) Abaco delle Murature della Regione Toscana.
- [22] (n.d.) Laterizi comuni, mattoni e forati. La Moderna Laterizi.
- [23] (2019) Istruzioni per l'applicazione Dell'«Aggiornamento Delle “Norme Tecniche per Le Costruzioni”» Di Cui al Decreto Ministeriale 17 Gennaio 2018.